Available online at www.sciencedirect.com

ScienceDirect

Procedia Engineering 70 (2014) 429 – 438

Procedia Engineering

www.elsevier.com/locate/procedia

12th International Conference on Computing and Control for the Water Industry, CCWI2013

Landslide tsunami: physical modeling for the implementation of tsunami early warning systems in the Mediterranean Sea

P. De Girolamo[a], M. Di Risio[b,*], A. Romano[c], M.G. Molfetta[d]

[a]*University of Rome La Sapienza, DICEA, Dept. of Civil, Constructional and Environmental Engineeering, Via Eudossiana 18, 00184 Rome, Italy*
[b]*University of L'Aquila, DICEAA, Civil, Dept. Construction-Architectural and Environmental Engineering, Environmental and Maritime Hydraulic Laboratory, P.le Pontieri 1, 67040 Monteluco di Roio, L'Aquila, Italy*
[c]*University of Roma Tre, Dept. of Engineering, Via Vito Volterra 62, 00146, Roma, Italy*
[d]*Technical University of Bari, DICATECh, Dept. of Civil, Environmental, Building Engineering and Chemistry, Coastal Engineering Laboratory (LIC), Area Universitaria di Valenzano - S.P. Valenzano Casamassima, Km.3 - 70010 Valenzano (Bari)*

Abstract

The main difficulty in implementing a Tsunami Early Warning System (TEWS) in the Mediterranean Sea arises from the proximity of the tsunami sources to the coasts at risk. Between few minutes and few tens of minutes are available for a timely warning of a possible approaching tsunami. To date, the only TEWS already operating in the Mediterranean Sea is that run by the Italian Department for Civil Protection at the Island of Stromboli, located north of Sicily in the south of the Tyrrhenian Sea. An active volcano is located on the island. The landslides that often detach from the "Sciara del Fuoco" following eruptive activity may result in the generation of tsunamis that propagate around the island and toward the coasts of Italy. The implemented TEWS is therefore aimed at mitigating the risk of landslide generated tsunamis.

The present paper illustrates some of the experimental activities carried out during the last decade aimed at improving the TEWS of Stromboli island. A series of experiments was carried out with the main aim of gaining insight on landslide generated tsunamis. In general, the experimental results were intended to be useful for the definition of forecasting formulae, for the validation of mathematical models, for the improvement of the knowledge on involved phenomena and for the optimization of detection algorithm. In particular, the physical investigations aimed at improving the TEWS of the Stromboli are detailed.

Keywords: Landslide Tsunami; tsunami early warning systems; physical modeling

1. Introduction

The actions to be taken in order to mitigate the effect of natural phenomena can be listed referring to the interval between the time they are actually taken and the time of the natural phenomenon occurrence. In this respect, these actions can be identified as:

* Corresponding author. Tel.: +39-(0)862-434534 ; fax: +39-(0)862-434554.
E-mail address: marcello.dirisio@univaq.it

doi:10.1016/j.proeng.2014.02.048

- preventive actions, i.e that are taken previously to the natural phenomenon occurrence;
- almost simultaneous actions, i.e. those taken at the natural phenomenon occurrence on the basis of the warning given by an effective Early Warning Systems (EWS);
- following actions, or actions taken after the occurrence of the natural phenomenon, i.e. aid actions.

In Italy, the national agency responsible for natural disaster mitigation is the Department for Civil Protection (DPC) run by the Presidency of the Italian Council of Ministers. The DPC is leaded by the Head of the Department who acts under the direct responsibility of the President of the Council of Ministers. It is responsible of providing the territorial local authorities with guidelines that - depending on the considered natural phenomenon - should be followed in order to take actions in advance and after the occurrence of the possible events. Furthermore, DPC is directly in charge of the actions to be taken at the time of event occurrence and, in particular, of the implementation of effective Early Warning Systems.

As far as the tsunamis are concerned, general guidelines referring to the actions to be taken in advance and after the time of occurrence of the phenomenon does not exist yet in Italy. Nevertheless the Italian DPC developed a highly effective rescue-organization system (i.e following actions) capable of facing also tsunami events. This system is commonly considered, for its organization, for its emergency and rescue equipment, and for its highly qualified staff, one of the best in the world. The main difficulty in implementing a Tsunami Early Warning System (TEWS) in the Mediterranean Sea arises from the proximity of the tsunami sources to the coasts at risk. Between few minutes and few tens of minutes are in fact available for a timely warning of a possible approaching tsunami. A further difficulty is of political nature. Indeed it is necessary the cooperation between the 16 countries that gives onto the Mediterranean Sea, as only seven of them belong to the European Community. In order to address issues related to the tsunami waves in Mediterranean sea, in 2005 the Intergovernmental Oceanographic Commission of UNESCO (IOC-UNESCO) received a mandate from the international community to coordinate the establishment of a Tsunami Early Warning and Mitigation System in the North-East Atlantic, the Mediterranean and connected seas (ICG/NEAMTW).

At present, the only TEWS already operating in the Mediterranean Sea is that run by DPC at the Island of Stromboli, located north of Sicily in the south of the Tyrrhenian Sea. An active volcano is located on the island. A significant geological feature of the volcano is the 'Sciara del Fuoco' (Stream of fire), a big horseshoe-shaped depression on the northwestern flank of the volcanic cone. The landslides that often detach from the 'Sciara del Fuoco' following eruptive activity may result in the generation of tsunamis that propagate around the island and toward the coasts of Italy. The implemented TEWS is therefore aimed at mitigating the risk of landslide generated tsunamis. Several Italian researchers work in the field of tsunamis, studying the mechanics of either generation or propagation, or the possible means of detection. These researchers work within either Universities or National Research Agencies such as the National Agency for Geophysics and Volcanology that is in particular responsible for the Italian Seismographic Network.

The present paper aims at reporting an overview of some experimental research activities useful to improve the TEWS of Stromboli island. Indeed, the events occurred on December 30, 2002 at Stromboli island motivated a series of three-dimensional experimental works aimed at reproducing the wave generation by semi-elliptical landslides at straight coast and conical islands. Firstly, a series of experiments was carried out in a three-dimensional wave tank where a plane beach was placed. Along the beach a semi-elliptical solid landslide model were left to slide along the incline by generating impulse waves. Both partially submerged and subaerial landslide were reproduced. The experimental results were used as starting point for a further three-dimensional experimental investigation aimed at reproducing impulse waves propagation around a conical island placed at the centre of a large wave tank (50 m long, 30 m wide, 3 m high). The induced run-up along the coast was measured by means of special gauges directly embedded into the island flanks. Only subaerial landslides were reproduced and the role of undisturbed shoreline radius was investigated. The same experimental layout was used in order to collect not only the induced wave runup, but also the free surface elevation related to the wave pattern propagating around the island.

2. Physical modeling of landslide generated waves

In the present work subaerial landslides are considered; thus, we focus mainly on this kind of generation mechanisms. When a subaerial landslide hits the water boundary and, consequently, enters the water, the sliding mass

interacts with the water body and transfers its energy to it; a tsunami is then triggered. The generated impulse waves both radiate seaward and propagate alongshore. In such a case trapped waves can take place and propagate along the coast by inducing large wave run-up, observed in some real cases (Ursell, 1952, Liu and Yeh, 1996, Liu et al., 1998, Johnson, 2007, Di Risio et al., 2009a). A clear, although qualitative, description of the generation physics has been provided by Liu et al. (2005), Di Risio et al. (2009a) and Di Risio et al. (2011). The latter authors stated that "When landslide enters the water body, it pushes ahead the fluid and a leading positive seaward radiating wave is generated. Once the landslide becomes totally submerged, the water is initially depressed by generating a trailing wave through. Strong alongshore free surface gradients occur in the generation area resulting in converging flows that collide and rebound along the centreline of the landslide. The rebound is the responsible of a large positive wave radiating offshore".

Several researches have been carried out aiming at shedding light on the features of the landslide-generated waves (e.g. Kamphuis and Bowering, 1970, Walder et al., 2003, Panizzo et al., 2005a, Di Risio and Sammarco, 2008). However, it has to be mentioned that most of the works cited so far mainly aim at studying the features of the waves that, leaving the generation area, radiate seaward. Indeed, aiming at implementing a Tsunami Early Warning System (TEWS) in the Mediterranean Sea, it can be more interesting to look at those waves that propagate alongshore for long distances, inundating the coasts. The physics of the wave propagation alongshore is dominated by complex phenomena (i.e., refraction, diffraction, reflection, etc.); in a qualitative way it is possible to state that the wave propagation alongshore is intimately related to the so-called "tsunamis trapping mechanisms". The first studies on the tsunamis propagation alongshore have been carried out in the last decades. Many authoritative experimental, numerical and analytical studies have been addressed the propagation of the landslide-generated waves both along straight coasts (e.g. Yeh, 1985, Chang, 1995, Liu and Yeh, 1996, Liu et al., 1998, Lynett and Liu, 2005, Sammarco and Renzi, 2008, Di Risio et al., 2009a, Renzi and Sammarco, 2012, Seo and Liu, 2013) and around circular islands (e.g. Yeh et al., 1994, Tinti and Vannini, 1994, 1995, Cho and Liu, 1999, Liu et al., 2005, Di Risio et al., 2009b, Renzi and Sammarco, 2010). It is demonstrated that edge waves (i.e., trapped waves) dominate the wave propagation along the shore, when a straight beach is considered. More complex is the physics of the wave propagation alongshore as far as a circular island is concerned, as pointed out by Renzi and Sammarco (2010). The latter authors demonstrated that in a polar-symmetric topography a perfect wave trapping is not possible.

In the followings sections the main results of two series of experiments are discussed. The mentioned experimental campaigns aimed at shedding light on the features of the landslide-generated tsunamis that occur at a straight coast and at a conical island respectively. A brief description of the experimental setup and of the main research findings is provided accordingly.

2.1. Straight coasts

In this section the features of the landslide-generated tsunamis that occur at a straight coast are presented. A more complete description of the experimental finding can be found in Di Risio et al. (2009a). Di Risio et al. (2009a) carried out a series of experiments in a three-dimensional wave tank aiming at reproducing landslide-generated tsunamis at a straight beach. The experiments have been carried out at the Environmental and Maritime Hydraulic Laboratory (LIAM) of the University of L'Aquila (Italy) in a three-dimensional wave tank (10.8 m long and 5.5 m wide). The maximum water depth is of 0.80 m. The physical model is shown in Figure 1 (left). Along two of the four tank sides an overspill has been deployed in order to reduce the reflection of the waves and to fix the maximum water level. A sloping beach has been placed along the long side of the tank. The steepness of the slope is 1/3 (1 vertical, 3 horizontal). The beach is built in PVC sheets, and it is sustained by a steel frame. The cross-shore section is made of a sloping part and of a constant-depth part 2.15 m long. It is worth to mention that the experimental layout is similar to that simulated numerically by Lynett and Liu (2005), although the beach was steeper in the experimental layout. The landslide model is a rigid body and is shaped as a half of an ellipsoid. In a reference frame with the origin placed at the centre of the ellipsoid, the landslide models are described by the following equation:

$$x^2/a^2 + y^2/b^2 + z^2/c^2 = 1 \tag{1}$$

where x is the coordinate directed along the incline, y the coordinate parallel to the undisturbed shoreline and z is the orthogonal distance from beach flank. The axis a (orthogonal to the undisturbed shoreline) is equal to 0.40 m (landslide length $2a = 0.80$ m), the axis b (parallel to the undisturbed shoreline) is equal to 0.20 m (landslide width

Fig. 1. Picture of the straight coast physical model (left) and of the conical island (right).

$2a$ = 0.40 m), the axis c (orthogonal to the island flank) is equal to 0.05 m (landslide thickness). The density of the landslide models was kept constant to 1.83 kg/m^3 for a total mass of about 15.4 kg. The using of solid (i.e. not granular) aims at observing the worst scenario (e.g. Di Risio et al., 2011). In order measure the displacement of the landslide model an accelerometer has been placed inside the model itself. As the focus of the work of Di Risio et al. (2009a) was mostly on the runup along the coast, special wave gauges have been built by employing two steel bars (square section of 4 *mm* × 4 *mm*) directly embedded into the PVC of the slope to measure the instantaneous movements of the shoreline

The experimental study has been carried out by reproducing both subaerial and partially submerged landslides. Furthermore the experiments aimed at evaluate the influence of the dropping height ζ in terms of the generated waves. It is worth to highlight that the experimental layout allowed to observe the near field wave pattern, by using a high resolution image analysis, and the propagation alongshore of the leading wave before the sidewalls reflection contaminated the induced waves, by using the run-up measurements.

The analysis of the near field pointed out that for partially submerged landslides the shoreline appears V-shaped. For subaerial landslides the body pushes strongly away the water resulting in a deep U-shaped shoreline. All the waves recorded in the experiments performed by Di Risio et al. (2009a) always had first a crest and then a trough. As the waves propagate away from the generation area the crest tends to become smaller than the trough and the period of the waves increases.

As far as the maximum runup is concerned, it appeared that in the far field it was almost always induced by the second or by the third wave. Furthermore, it is demonstrated that only very close to the generation area the first wave is responsible of the maximum runup. On the contrary the minimum rundown is almost always given by the trough of the first wave. Moreover, by estimating the celerity of the first wave it appeared that the celerity grows as the wave propagates along the coast. Furthermore the celerity at which the crest propagates is larger than that of the trough, consistently with the observed increase of the period.

2.2. *Conical islands*

In this section the features of the landslide-generated tsunamis that occur at a conical island are presented and discussed. It has to be mentioned that an exhaustive description can be found in the works of Di Risio et al. (2009b) and Molfetta et al. (2010). The experiments have been carried out in a large wave tank (50 m long, 30 m wide, 3 m deep) at the Research and Experimentation Laboratory for Coastal Defense of Polytechnic of Bari (LIC, Italy). The physical model consists of a truncated conical island with base diameter equal to 8.90 m and maximum height equal to 1.20 m made up of PVC sheets (thickness 0.01 m) sustained by a rigid steel frame (see Figure 1, right). The island is placed at the centre of the tank in order to obtain an appropriate distance from the tank walls; indeed, the walls when are reached by radiating waves induce spurious reflected waves that contaminate the experimental domain. The water depth was kept constant to 0.80 m. The slope (α) of the island flanks is of $\cot\alpha = 3$ (i.e. 1 vertical, 3 horizontal) to reproduce the typical slope of volcanic islands where landslides are likely to occur (i.e. Stromboli Island, Southern Tyrrhenian Sea, Italy, Tinti et al. (2005)). One of the island flanks reproduces a slide that allows landslide model to slide along the island and to enter the water; thus tsunamis can be triggered. Notwithstanding the physical model reproduces a geometry as general as possible, it is interesting to highlight that the conical island could

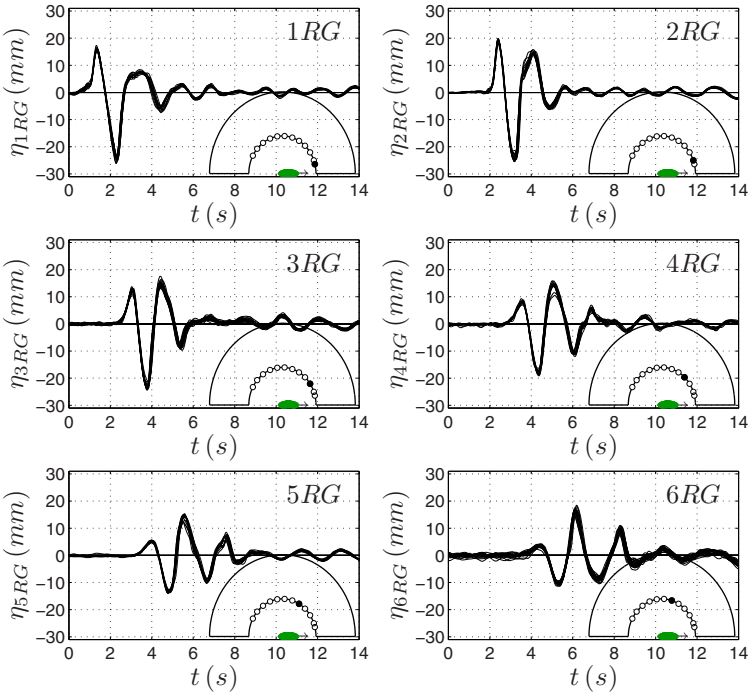

Fig. 2. Superposition of all the run-up time series (LS2).

be a schematized (and idealized) reproduction of the Stromboli Island, if a Froude law scale 1:1000 is considered. Accordingly the slide along the island flanks can be seen as a reproduction of the Sciara del Fuoco.

During the experiments two different landslide models have been used. These models are rigid bodies and they are shaped as a half of an ellipsoid similar to that used during the straight coast experiments. The first one (hereinafter referred to as LS1) is characterized by a thickness of 0.05 m (c=0.05 m). The LS1 volume is then equal to V = 0.0084 m^3. It is worth to highlight that LS1 is the same landslide body used during the straight coast experiments detailed in the previous section. The thickness of the second landslide model (hereinafter referred to as LS2) is 0.10 m (c=0.10 m) and the volume V = 0.0168 m^3. The density of the landslide models was kept constant to 1.83 kg/m^3 for a total mass of about 15.4 kg and 31.7 kg for LS1 and LS2 respectively.

The experiments aim at measuring the waves generated by the landslide model that slides down the island flank. A high-resolution camera was placed on a steel frame placed just outside of the wave tank, directly in front of the generation area. The digital images collected by means of the video-camera have been used to reconstruct the landslide motion. Given that the measurements aim at forming a benchmark to validate theoretical model, a large number of instruments have been used to measure the free surface elevation (we refer to the work of Romano (2013) for further details). In order to measure the free surface elevation time series around the conical island wave gauges (hereinafter referred to as WG), ultrasonic water level sensors (hereinafter referred to as US) and run-up gauges (hereinafter referred to as RG) were employed.

Some of the instruments were kept fixed in space (to check the repeatability of the experiments), some others were placed on a steel frame that can rotate around the island centre spanning a half of the island (to measure the whole wave pattern around the island). This "movable" system allows to collect the free surface time series along cross-shore sections, starting from the axis along which the landslide moves (θ =0°) up to the rear side of the island (θ =180°). For each test, the landslide is placed at starting position and the movable steel frame moved to the correct angular position, then the acquisition process begins, the landslide model is released and the tsunami is generated. Typically the acquisition process is stopped about 50 s after the release of the landslide, when the waves reflected at the side walls had completely contaminated the wave field. The procedure was repeated for each position of the movable frame, from θ =0° up to θ =180° every 5°, for a total of 37 landslide releases.

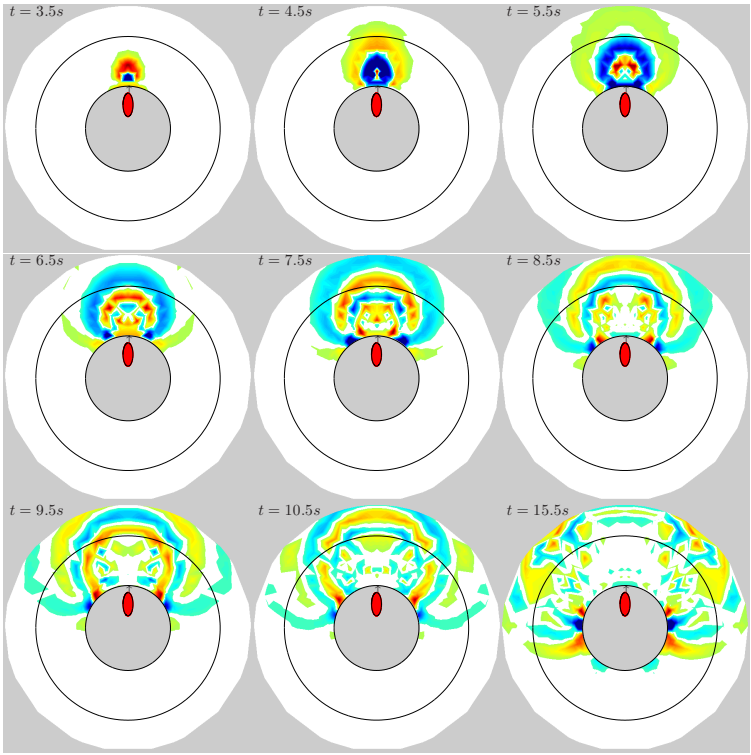

Fig. 3. Free surface elevation around the island at several time steps from the landslide release (LS1). Note: in order to magnify the features of the wave propagation, different color scales have been used for each panel.

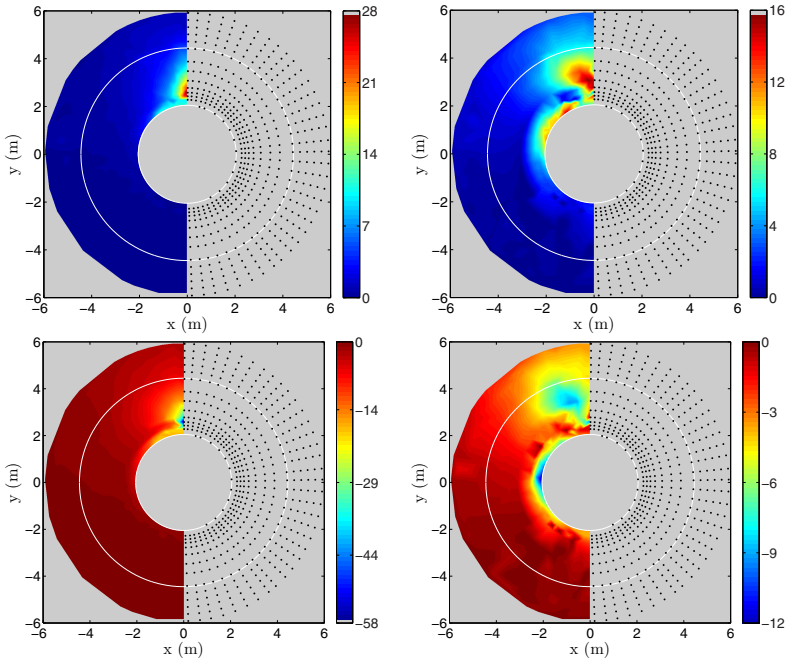

Fig. 4. Spatial distribution of crest and trough amplitudes around the island (LS1). Left panels: first wave. Right panels: second wave. Upper panels: wave crests. Lower panels: wave troughs. Note: colorbars are expressed in mm.

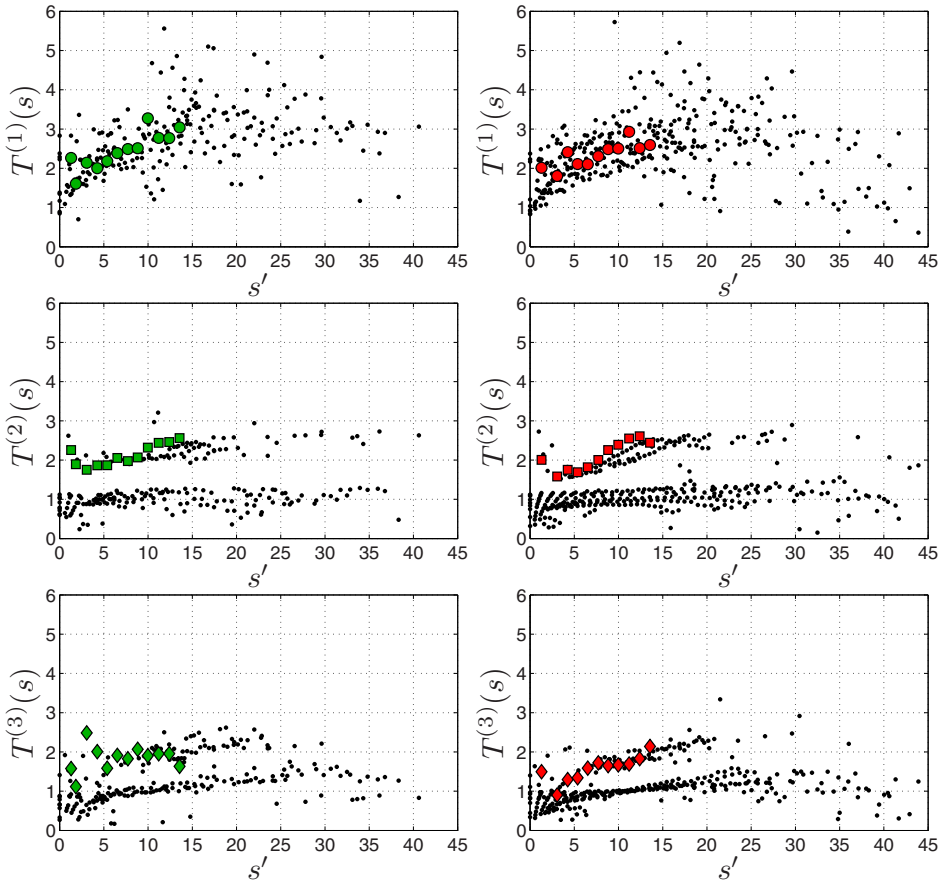

Fig. 5. Individual wave periods of the first three waves measured by the moving arm and the run-up gauges (LS1, right panels; LS2, left panels). Note : black points refer to the wave periods of the waves measured by the moving arm, while the solid markers (green and red) refer to the wave periods of the run-up waves.

Figure 2 shows the superposition of the run-up time series obtained from the LS2. It has to be mentioned that since a large number of repetitions have been carried out in order to measure the wave propagation around the whole island by means of movable sensors, then a repeatability analysis has to be performed to ensure that the results are meaningful. We refer to Romano (2013), in which a statistical repeatability analysis has been carried out, for further details. The analysis of the runup gauges measurements raises several points of discussions. As highlighted by Di Risio et al. (2009b), the crest amplitude of the waves first increases with the distance from the generation area and then decreases. Figure 2 shows that the crest of the first wave of the packet becomes very high close to the landslide area in which it induces the maximum runup; then the second wave becomes more important, and for a certain distance it induces the largest inundation. Then the third wave grows and becomes the highest, and so on. This is the typical behavior of frequency dispersive waves.

Once the experimental repeatability has been quantitatively estimated, by analyzing the data of the fixed gauges (i.e., RGs), it is possible to use the measurements collected by the movable system. In Figure 3 the free surface elevation contour plots, evaluated at several time steps since the landslide has been released, are represented. Each contour plot has been obtained by linearly interpolating the free surface elevation, collected around the island, at a given time step. It is shown that the spatial resolution of the measurements is high enough to describe in depth the tsunamis propagation around the island (both alongshore and in deep water area).

Figure 3 clearly shows that in the first phases, after the landslide impact, the waves mainly propagate seaward (i.e., radiating waves), while, as the time increases, it seems clear that the tsunami propagates alongshore and inundate the

island coast. This suggests that tsunamis trapping mechanisms, due to bathymetry, play a fundamental role in the propagation/inundation phenomena. Furthermore it appears that the high spatial resolution measurements provide an effective tool for gaining insight on the wave propagation phenomena, and, consequently to form a benchmark.

As far as the free surface elevation time series collected around the island are concerned a more complete picture of the overall wave field can be depicted. A more detailed description of wave pattern can be addressed by looking at the spatial distribution of crest and trough amplitudes around the island. Figure 4 shows the spatial distribution of the wave crest (upper panels) and trough amplitudes (lower panels) of the first (left panels) and second wave (right panels) obtained by linearly interpolating the experimental data obtained by using LS1. As far as the wave crest and trough amplitudes of the first wave are concerned (left panels), the highest amplitudes occur in front of the generation area. Furthermore in Figure 4 it is shown that the energy of the first wave (both wave crest and trough) seems to be channeled in a direction that is parallel to the one along which the landslide travels, while as the angular distance ϑ from the generation area grows the wave crest and trough amplitudes rapidly decrease. By observing the spatial structure of the second wave (right panels of the Figure 4) other interesting features can be catched. As shown in Figure 4, the maximum amplitude of the first wave crest occurs close to the impact point, while the trailing first wave trough amplitude and, in particular, second wave crest and trough amplitudes occur at increasing distance, in front of the generation area. Actually the first wave crest and trough can be interpreted as a near-field effect of the wave generation, being the crest generated by the piston-like generation mechanism occurring when the landslide enters the water and the trough generated by the rebound of water and by the interaction of landslide tail with the free surface. As the distance from the generation area increases the effects of the generation mechanism becomes less important and the wave pattern is governed by propagation mechanisms. It is important to stress that only when the propagation mechanisms become important, the maximum amplitudes occur at the coast as already observed in the case of straight coast by Lynett and Liu (2005) and Di Risio et al. (2009a). This is due to frequency dispersion which characterizes the propagation of the seaward radiated waves as well as the propagation of the ones that travel alongshore.

Finally it is interesting to consider the features of the wave period. As far as the individual first three waves of the generated train are concerned, Figure 5 shows the wave periods of the waves measured by means of both the moving arm and the run-up gauges, as a function of the dimensionless variable s', defined as follows

$$s' = \frac{r_0 \vartheta}{b}, \tag{2}$$

where $r_0 = 2.05$ m is the radial distance that identifies the undisturbed shoreline, ϑ is the angular position around the island and $b = 0.40$ m is the landslide width. The black points refer to the wave periods of the waves measured by the moving arm, while the solid markers (green and red) refer to the wave periods of the run-up waves. It is almost clear that the first wave period, even if rather dispersed, increases as the distance from generation area grows. The periods of the trailing waves exhibit lower dispersion and it is possible to observe clear differences between radiating waves period and the period of the waves that propagate along the coast of the island, with the former lower than the latter. It can be argued that two different wave system occurs and each of them obeys to their own dispersion relation.

3. Improvement of TEWSs

The main Tsunami Early Warning Systems (TEWSs) component rely on seismic monitoring or ground-movement monitoring network of probable tsunami sources in order to perform a fast detection of possible tsunamigenic sources. Indeed, it has to be stressed that, even if great efforts have been undertaken in developing new technologies (e.g. Hamlington et al., 2011, Chierici et al., 2010, Sammarco et al., 2013), at present only direct detection in sea-level measurements can confirm its actual generation and propagation (e.g. Bellotti et al., 2009, Bressan and Tinti, 2011, 2012).

Experimental findings briefly detailed in the previous sections have been used in order to improve Tsunami Early Warning Systems and to optimize them on the light of the generation and propagation mechanisms. In particular, the optimization of the TEWS rely on the correct layout of the sea-level monitoring network (i.e. the preventive actions as defined in section 1). Furthermore the experimental results may be precious to identify the areas prone to be inundated (i.e. almost simultaneous actions as defined in section 1) and the safe distance from the coast where collection points have to be located (i.e. following actions as defined in section 1).

Radiating waves propagate faster than the edge-waves like traveling along the coast (i.e. short alarm delay), but they may me hardly detectable by standard pressure sensors as they propagate as almost deep water waves. If coastal sensors are considered the available time to spread alarm may be low. Then, experimental results suggest that both off- and near-shore sensors should be deployed in order to make the TEWS more effective (Bellotti et al., 2009). Moreover, the experimental results were selected as benchmark data-sets for the validation of mathematical models useful within the framework of a TEWS in both the real time and design stage. Indeed, Cecioni et al. (2011) proposed an inversion procedure (validated against experimental data) based on the numerical solution of the linearized mild-slope equation (Bellotti et al., 2008, Cecioni and Bellotti, 2010b,a) suitable for the real-time forecasting of the landslide tsunami induced inundation based on the use of partial (i.e. real-time) free surface time series. This is the case, other than the direct detection of tsunami occurrence, for which the availability of suitable time series are needed, i.e. tsunami detection algorithms have to implemented in the software of the sensors (e.g. Beltrami, 2008, 2011, Beltrami and Di Risio, 2011, Bressan and Tinti, 2011, 2012). In order to define the inundation areas, the real-time procedure may be coupled to a near field modeling. Indeed, Montagna et al. (2011) showed that the commercial code FLOW-3D appears to be very effective for the reproduction of landslide tsunami generation. The validated numerical results reveal that it can be considered very accurate, both for the computation of runup (i.e. for the production of inundation maps), both for the forecast of the offshore-propagating waves. In view of the good accuracy of the results, the model has been applied to run a set of numerical tests that was not possible to perform in the laboratory, such as for example those involving fully submerged landslides.

4. Concluding remarks

The present paper reviews some of the experimental activities carried out during the last decade with the aim of improving the Tsunami Early Warning System in the case of landslide tsunami. A series of experiments carried out with the main aim of gaining insight on landslide generated tsunamis and to define a series of benchmark data-sets useful for (i) the validation of mathematical models, (ii) the improvement of the knowledge on involved phenomena and (iii) the optimization of detection algorithm are described. The main results of the experimental investigations are reviewed. The use of experimental findings to validate mathematical models and detection algorithm used within the frame of TEWSs are reported.

5. Acknowledgments

This work was carried out under the research projects PRIN2004 and PRIN2007 led by the first author and funded by the Italian Ministry for University and Scientific Research (MIUR). All the people involved in the physical modeling are acknowledged.

References

Bellotti, G., Cecioni, C., De Girolamo, P., 2008. Simulation of small-amplitude frequency-dispersive transient waves by means of the mild-slope equation. Coastal Engineering 55, 447–458.

Bellotti, G., Di Risio, M., De Girolamo, P., 2009. Feasibility of Tsunami Early Warning Systems for small volcanic islands. Natural Hazards and Earth System Sciences 9, 1911–1919.

Beltrami, G., 2008. An ANN algorithm for automatic, real-time tsunami detection in deep-sea level measurements. Ocean Engineering 35, 572–587.

Beltrami, G.M., 2011. Automatic, real-time detection and characterization of tsunamis in deep-sea level measurements. Ocean Engineering 38, 1677–1685.

Beltrami, G.M., Di Risio, M., 2011. Algorithms for automatic, real-time tsunami detection in wind-wave measurements Part I: Implementation strategies and basic tests. Coastal Engineering 58, 1062–1071. doi:10.1016/j.coastaleng.2011.06.004.

Bressan, L., Tinti, S., 2011. Structure and performance of a real-time algorithm to detect tsunami or tsunami-like alert conditions based on sea-level records analysis. Nat. Hazards Earth Syst. Sci 11, 1499–1521.

Bressan, L., Tinti, S., 2012. Detecting the 11 March 2011 Tohoku tsunami arrival on sea-level records in the Pacific Ocean: application and performance of the Tsunami Early Detection Algorithm (TEDA). Nat. Hazards Earth Syst. Sci 12, 1583–1606.

Cecioni, C., Bellotti, G., 2010a. Inclusion of landslide tsunamis generation into a depth integrated wave model. Nat. Hazards Earth Syst. Sci 10, 2259–2268.

Cecioni, C., Bellotti, G., 2010b. Modeling tsunamis generated by submerged landslides using depth integrated equations. Applied Ocean Research 32, 343–350.

Cecioni, C., Romano, A., Bellotti, G., Di Risio, M., de Girolamo, P., 2011. Real-time inversion of tsunamis generated by landslides. Nat. Hazards Earth Syst. Sci 11, 2511–2520.

Chang, K.T., 1995. Evolution of landslide-generated edge wave packet. Ph.D. thesis. University of Washington.

Chierici, F., Pignagnoli, L., Embriaco, D., 2010. Modeling of the hydroacoustic signal and tsunami wave generated by seafloor motion including a porous seabed. Journal of Geophysical Research: Oceans (1978–2012) 115.

Cho, Y.S., Liu, P.L.F., 1999. Crest-length effects in nearshore tsunami run-up around islands. J. Geophys. Res. 104, 7907–7913. doi:10.1029/1999JC900012.

Di Risio, M., Bellotti, G., Panizzo, A., De Girolamo, P., 2009a. Three-dimensional experiments on landslide generated waves at a sloping coast. Coastal Engineering 56, 659–671. doi:10.1016/j.coastaleng.2009.01.009.

Di Risio, M., De Girolamo, P., Bellotti, G., Panizzo, A., Aristodemo, F., Molfetta, M.G., Petrillo, A.F., 2009b. Landslide-generated tsunamis runup at the coast of a conical island: New physical model experiments. Journal of Geophysical Research-Oceans 114. doi:10.1029/2008JC004858.

Di Risio, M., De Girolamo, P., Beltrami, G., 2011. Forecasting landslide generated tsunamis: a review, in: Tsunami, Research and Technologies. Intech, pp. 81–106.

Di Risio, M., Sammarco, P., 2008. Analytical modeling of landslide-generated waves. Journal of waterway, port, coastal, and ocean engineering 134, 53–60.

Hamlington, B., Leben, R., Godin, O., Legeais, J., Gica, E., Titov, V., 2011. Detection of the 2010 Chilean tsunami using satellite altimetry. Nat. Hazards Earth Syst. Sci 11, 2391–2406.

Johnson, R.S., 2007. Edge waves: theories past and present. Philosophical Transactions Of The Royal Society A-Mathematical Physical And Engineering Sciences 365, 2359–2376. doi:10.1098/rsta.2007.2013.

Kamphuis, J., Bowering, R., 1970. Impulse waves generated by landslides, in: Proceedings of the International Conference on Coastal Engineering, pp. 575–588.

Liu, P., Wu, T., Raichlen, F., Synolakis, C., Borrero, J., 2005. Runup and rundown generated by three-dimensional sliding masses. Journal of fluid Mechanics 536, 107–144.

Liu, P., Yeh, H., 1996. The generation of edge waves by a wave-maker. Physics Of Fluids 8, 2060–2065. doi:10.1063/1.869008.

Liu, P., Yeh, H., Lin, P., Chang, K., Cho, Y., 1998. Generation and evolution of edge-wave packets. Physics Of Fluids 10, 1635–1657. doi:10.1063/1.869682.

Lynett, P., Liu, P., 2005. A numerical study of the run-up generated by three-dimensional landslides. Journal of Geophysical Research-Oceans 110. doi:10.1029/2004JC002443.

Molfetta, M., Di Risio, M., Romano, A., Bellotti, G., Pratola, L., De Girolamo, P., Damiani, L., 2010. Tsunamis generated by subaerial landslides at the coast of conical islands: a new set of high resolution experimental dataset, in: Proceedings of the Third International Conference on the Application of Physical Modelling to Port and Coastal Protection: Coastlab 10, Barcelona, Spain, International Coastal Resources Research Centre (CIIRC). pp. 1–10.

Montagna, F., Bellotti, G., Di Risio, M., 2011. 3D numerical modeling of landslide-generated tsunamis around a conical island. Natural hazards 58, 591–608.

Panizzo, A., De Girolamo, P., Petaccia, A., 2005a. Forecasting impulse waves generated by subaerial landslides. Journal of geophysical research 110, C12025.

Renzi, E., Sammarco, P., 2010. Landslide tsunamis propagating around a conical island. Journal of Fluid Mechanics 650, 251–285. doi:10.1017/S0022112009993582.

Renzi, E., Sammarco, P., 2012. The influence of landslide shape and continental shelf on landslide generated tsunamis along a plane beach. Nat. Hazards Earth Syst. Sci 12, 1503–1520.

Romano, A., 2013. Physical and numerical modelling of landslide-generated tsunamis at a conical island: generation, propagation and early warning. Ph.D. thesis. University of Roma Tre.

Sammarco, P., Cecioni, C., Bellotti, G., Abdolali, A., 2013. Depth-integrated equation for large-scale modelling of low-frequency hydroacoustic waves. Journal of Fluid Mechanics 722, R6.

Sammarco, P., Renzi, E., 2008. Landslide tsunamis propagating along a plane beach. Journal of Fluid Mechanics 598, 107–119. doi:10.1017/S0022112007009731.

Seo, S.N., Liu, P.L.F., 2013. Edge waves generated by the landslide on a sloping beach. Coastal Engineering 73, 133–150.

Tinti, S., Manucci, A., Pagnoni, G., Armigliato, A., Zaniboni, F., 2005. The 30 December 2002 landslide-induced tsunamis in Stromboli: sequence of the events reconstructed from the eyewitness accounts. Natural Hazards and Earth System Science 5, 763–775.

Tinti, S., Vannini, C., 1994. Theoretical investigation on tsunamis induced by Seismic Faults near Ocean Islands. Marine Geodesy 17, 193–212. doi:10.1080/15210609409379727.

Tinti, S., Vannini, C., 1995. Tsunami trapping near-circular islands. Pure And Applied Geophysics 144, 595–619. doi:10.1007/BF00874385.

Ursell, F., 1952. Edge Waves on a Sloping Beach. Proceedings of the Royal Society of London. Series A. Mathematical and Physical Sciences 214, 79–97. doi:10.1098/rspa.1952.0152.

Walder, J.S., Watts, P., Sorensen, O.E., Janssen, K., 2003. Tsunamis generated by subaerial mass flows. Journal of geophysical research 108, 2236.

Yeh, H., 1985. Nonlinear progressive edge waves - their instability and evolution. Journal of Fluid Mechanics 152, 479–499. doi:10.1017/S0022112085000799.

Yeh, H., Liu, P.L.F., Briggs, M., Synolakis, C.E., 1994. Propagation and amplification of tsunamis at coastal boundaries. Nature 372, 353–355. doi:10.1038/372353a0.